ELSEVIER

Agricultural and Forest Meteorology 105 (2000) 55–68

AGRICULTURAL AND FOREST METEOROLOGY

www.elsevier.com/locate/agrformet

Spatial and temporal dynamics of vegetation in the San Pedro River basin area

J. Qi [a,*], R.C. Marsett [b], M.S. Moran [b], D.C. Goodrich [b], P. Heilman [b], Y.H. Kerr [c], G. Dedieu [c], A. Chehbouni [d], X.X. Zhang [e]

[a] *Department of Geography, Michigan State University, 315 Natural Science Building, East Lansing, MI 48824-1115, USA*
[b] *USDA–Agricultural Research Service, Tucson, AZ, USA*
[c] *CESBIO, Toulouse, France*
[d] *IRD/IMADES, Hermosillo, Mexico*
[e] *Center for Space Science, Applied Research, Chinese Academy of Science, Beijing, China*

Abstract

Changes in climate and land management practices in the San Pedro River basin have altered the vegetation patterns and dynamics. Therefore, there is a need to map the spatial and temporal distribution of the vegetation community in order to understand how climate and human activities affect the ecosystem in the arid and semi-arid region. Remote sensing provides a means to derive vegetation properties such as fractional green vegetation cover (f_c) and green leaf area index (GLAI). However, to map such vegetation properties using multitemporal remote sensing imagery requires ancillary data for atmospheric corrections that are often not available. In this study, we developed a new approach to circumvent atmospheric effects in deriving spatial and temporal distributions of f_c and GLAI. The proposed approach employed a concept, analogous to the pseudoinvariant object method that uses objects void of vegetation as a baseline to adjust multitemporal images. Imagery acquired with Landsat TM, SPOT 4 VEGETATION, and aircraft based sensors was used in this study to map the spatial and temporal distribution of fractional green vegetation cover and GLAI of the San Pedro River riparian corridor and southwest United States. The results suggest that remote sensing imagery can provide a reasonable estimate of vegetation dynamics using multitemporal remote sensing imagery without atmospheric corrections.

Keywords: Remote sensing; Spatial and temporal dynamics; San Pedro River basin; Fractional cover; Green leaf area index

1. Introduction

Climate change and increasing human activities have resulted in a substantial change in the vegetation type and distribution in the southwest United States. Chihuahuan desert shrubs and mesquite trees increasingly have become dominant and replaced native grasses over large areas (Kepner et al., 1998; Watts et al., 1998). The change in vegetation pattern has a feedback influence on the local and regional climate by reducing evaporative water losses from surface to atmosphere. Therefore, the spatial and temporal distributions of vegetation characteristics is important in understanding how climate and human activities affect the ecosystem in the semi-arid environment.

Estimation of vegetation properties with remotely sensed imagery has been quite successful. However, when applied to satellite imagery, tremendous

* Corresponding author. Tel.: +1-517-353-8736; fax: +1-517-432-1671.
E-mail addresses: qi@pilot.msu.edu, qi@tucson.ars.ag.gov (J. Qi).

0168-1923/00/$ – see front matter
PII: S0168-1923(00)00195-7

processing efforts related to atmospheric and bidirectional corrections are needed. Although procedures to correct these effects are available, ancillary data about atmospheric conditions and bidirectional properties of the surface types are limited in both space and time. This has prevented satellite data from being used to quantify vegetation dynamics for practical applications. A common practical technique to correct atmospheric effect is dark-object subtraction (Chavez, 1988; Caselles and Garcia, 1989), which subtracts the minimum pixel values of a dark object found in a scene with an assumption that no energy is reflected from that dark object. However, in many cases, it is impossible to find a dark object within a scene that is large enough to occupy more than one single pixel, especially when coarse spatial resolution satellites are used. An alternative is to use pseudo invariant objects (PIOs) within a scene to convert digital numbers to radiance or reflectance values (Schott et al., 1988; Moran et al., 1996, 1997). PIOs are those objects whose reflectances are known and remain approximately constant throughout time and therefore can be used to "calibrate" multitemporal images.

Reflectance properties of most PIOs, however, vary with many factors such as surface conditions. When bare soil fields are used as PIOs, e.g., their reflectances vary with soil moisture content and surface roughness, which changes throughout the season because of the impact of rainfall events. Use of either a dark object or a PIO for atmospheric corrections will not correct for bidirectional effects. When an image is acquired at an oblique view, the reflectance properties of most objects including PIOs may vary substantially. Therefore, oblique viewing will introduce a constant bias when PIOs are used for atmospheric corrections. Noise associated with atmospheric and bidirectional effects will be magnified when calculating derivative products such as vegetation cover and biomass, especially over sparsely vegetated surfaces. Thus, it is critical that methods be developed to circumvent atmospheric and bidirectional effects. The objective of this study is to develop an alternative technique to derive remote sensing products such as fractional green vegetation cover (f_c) and leaf area index (LAI) that are less sensitive to atmospheric effect. Although viewing angles may introduce errors in estimated f_c and LAI, no attempt was made to correct bidirectional effects in this study.

2. Methodology

By definition, a PIO is an object whose reflectance properties are invariant throughout time. Examples of such objects are bare soil fields, airstrips, and highways. Therefore, multitemporal remote sensing images can be converted to surface reflectances by using a linear relationship between raw digital numbers on the image and the known reflectances of the PIOs found within the scene. The key assumption is that the object is invariant in terms of surface reflectance. This assumption, however, is not valid for most natural land surfaces because their reflectance properties are known to vary with many external factors such as surface conditions and sensor's viewing angles. Therefore, the fundamental assumption of invariance in reflectance fails in most cases, resulting in uncertainties in surface reflectance and its derived products.

There are other physical properties besides reflectances that are indeed invariant with time and surface conditions. Such physical properties include the presence of vegetation or green biomass. For example, a bare soil field, which is often used as a PIO, changes in surface reflectance with surface moisture condition, roughness, and sensor/sun-viewing angles. However, the fractional green vegetation cover (f_c) or green leaf area index (GLAI) does not vary with these factors. Therefore, the bare soil field is variant in surface reflectances but invariant in green vegetation cover or green biomass, allowing one to use this truly invariant property to calibrate the green cover product rather than to calibrate reflectance.

We thus designed an adjustment approach (Fig. 1), using true invariant properties of most land surfaces, to circumvent the atmospheric effect in the derivation of biophysical properties of land surfaces. The adjustment approach (Fig. 1) consists of three steps. The first step is to identify surface targets void of vegetation, analogous to PIOs, whose physical sizes are at least twice larger than the spatial resolution of the remotely sensed imagery used. Such objects may be areas of bare soil fields, airport runways, and highways. To differentiate these objects from traditional pseudo reflectance-invariant objects, these objects are termed here as objects void of vegetation (OVV). By definition, the fractional green cover and GLAI values of OVVs should be zero. However, due to atmospheric effect, the derived f_c and GLAI values

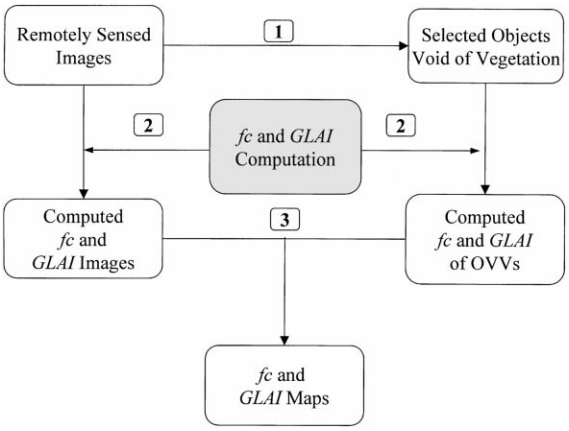

Fig. 1. Flow chart of the approach to compute green vegetation cover (f_c) and GLAI using OVVs.

of OVVs may not be zero and need to be adjusted. The second step is to compute this non-zero adjustment factor in terms of fractional cover and GLAI (algorithms for computing these two variables are described below). The third and final step is to compute the f_c and GLAI spatial distribution by subtracting the adjustment factor from the entire image.

In this study, we focused on the derivation of temporal dynamics of vegetation in the San Pedro River basin where the semi-arid land-surface-atmosphere (SALSA) program is currently focusing its effort (Goodrich et al., 2000). In particular, we used the proposed adjustment approach to derive spatial and temporal distributions of the fractional green vegetation cover (f_c) and GLAI of the study area. The selected OVVs in this study included the Wilcox playa, Arizona for all TM images and White Sands, New Mexico for the VEGETATION images. These OVVs can also be used as PIOs. The f_c and GLAI values of the Wilcox playa and White Sands were computed and subtracted from the entire f_c and GLAI images. The f_c and GLAI values of these OVVs provided baselines for each image to allow an automatic adjustment of the f_c and GLAI values from multitemporal remote sensing imagery.

2.1. Green vegetation cover estimate

Fractional green vegetation cover (f_c) in arid and semi-arid regions is an important variable in hydrological and ecological modeling studies. Their temporal dynamics and spatial distributions are often needed in global circulation models (GCMs) in order to compute the energy or water fluxes. Estimation of fractional green vegetation cover, f_c, from remotely sensed data is often associated with computation of spectral vegetation indices and their empirical relationships with fractional green vegetation cover. In this study, we used a linear mixing model to relate f_c with spectral vegetation indices.

Assume that a pixel signal consists of the contribution from two components: soil and vegetation. Let the fractional green vegetation cover be f_c and, therefore, the fractional soil cover would be $1 - f_c$. The resulting signal, S, as observed by a remote sensor can be expressed as

$$S = f_c S_v + (1 - f_c) S_s \tag{1}$$

where S_v is the signal contribution from the green vegetation component and S_s from the soil component. For pixels consisting of more than two components, Eq. (1) needs to be modified. This analysis assumed that a pixel consisted of only vegetation and soils. Eq. (1) can be applied to remotely sensed data in the reflectance domain (Maas, 1998) and in the spectral vegetation index domain (Zeng et al., 2000). When applied with a spectral vegetation index such as the normalized difference vegetation index (NDVI), Eq. (1) may be approximated by

$$\mathrm{NDVI} = f_c \times \mathrm{NDVI}_{veg} + (1 - f_c)\mathrm{NDVI}_{soil} \tag{2}$$

which can be re-written as

$$f_c = \frac{\mathrm{NDVI} - \mathrm{NDVI}_{soil}}{\mathrm{NDVI}_{veg} - \mathrm{NDVI}_{soil}} \tag{3}$$

where NDVI_{soil} is the NDVI value of an area of bare soil or OVV, and NDVI_{veg} is the NDVI value of a pure vegetation pixel.

Although many vegetation indices are available, we selected NDVI because of its traditional use in deriving vegetation variables. The NDVI_{soil} values should be constant throughout time and close to zero in theory for most type of bare soil surfaces. However, due to atmospheric effect, and changes in surface moisture conditions, NDVI_{soil} values vary substantially with time. In addition, they also vary from location to location because of difference in soil types and colors. Therefore, using a single value of NDVI_{soil} as a baseline

for the entire image may not be valid unless the area of interest consists of uniform soil types. For this reason, we selected surfaces near the center of an image to minimize errors associated with variations in NDVI values of OVVs. To use the proposed adjustment approach, it is not necessary to know the exact values of $NDVI_{soil}$ because this value will be computed from each image. The $NDVI_{soil}$ values from each image were used to compute the associated f_c and GLAI adjustment factors.

As previously stated, the spatial variation of bare soil surfaces may also be related to the sensor's observation angles. Therefore, depending on the sun-viewing geometry of each pixel, the selected $NDVI_{soil}$ may be different and thus result in uncertainties in f_c and GLAI estimation. To minimize the bidirectional effect, it is suggested to avoid large view angle data when nadir-looking images are available. In this study, the nadir-viewing TM images were used in the analysis. The proposed adjustment approach was designed to circumvent primarily the atmospheric effect, aiming at analyzing vegetation dynamics from multitemporal images. Uncertainties were expected when using images acquired with large viewing angle sensors.

The value for $NDVI_{veg}$ represents the maximum value of a fully vegetated pixel. Because of the temporally dynamic nature of green vegetation cover, this value needs to be empirically determined. In selecting such a value, we examined all images and selected an image acquired during the peak-growing season within the area of interest. The $NDVI_{veg}$ was determined in this study to be 0.8 from high spatial resolution data. During the selection process, surfaces of known to be 100% green cover were identified and the corresponding NDVI values were computed from multitemporal images, and then the highest value (0.8) was used for all image. This empirically determined value may also vary with atmospheric conditions (Kaufman and Tanre, 1992; Qi et al., 1994), which may cause some errors in the fractional cover computation in Eq. (3).

Because the NDVI is a ratio vegetation index, it can be directly computed with digital numbers, or with top of atmosphere radiance or reflectance, or surface reflectance. In this analysis, $NDVI_{veg}$ of 0.8 was determined using surface reflectances derived from TM images. When used with radiance, or digital numbers, or top-of-atmosphere reflectance or radiance, the $NDVI_{veg}$ may be different. However, once the data type (radiance, raw digital numbers, or top-of-atmosphere reflectance or radiance) is determined, the $NDVI_{veg}$ should be constant.

2.2. GLAI estimate

Another important vegetation characteristic is the GLAI. Unlike the fractional green vegetation cover, which is a two-dimensional horizontal variable, the GLAI is a variable describing the density of green vegetation. It is defined here as the total single-side area of green leaves per unit ground area. Therefore, its values can theoretically range from 0 to ∞, whereas f_c ranges from 0 to 1.

Approaches to derive GLAI exist using either empirical relationships with spectral vegetation indices or model inversion techniques. For arid and semi-arid regions such as the San Pedro River basin, we adapted the approach by Qi et al. (2000), which was derived using a combination of modeling and empirical approaches

$$\mathrm{GLAI} = a\,\mathrm{NDVI}^3 + b\,\mathrm{NDVI}^2 + c\,\mathrm{NDVI} + d \qquad (4)$$

where a, b, c, and d are empirical coefficients and were found to be $a = 18.99$, $b = -15.24$, $c = 6.124$, and $d = -0.352$ for arid and semi-arid regions. The GLAI values derived from these coefficients were validated using TM imagery data over a desert grassland, and therefore, the use of them over a large area of diverse vegetation remains to be further validated. Since the TM imagery used in this study covered the same geographic areas, it is expected that uncertainty in GLAI estimation from these coefficients would not be significantly different from the original study. Furthermore, if adjusted NDVI was used in Eq. (4), the coefficient d should be adjusted to zero to ensure that the GLAI values of OVV were zeros for all seasonal images.

3. Data description

3.1. Remote sensing data

Multitemporal images were acquired with Landsat TM, French SPOT 4 VEGETATION, and airborne sensors over the study area. They were geometrically

Table 1
Remote sensing images acquired in 1992, 1997, and 1998 over the study area in the southwest United States on different dates and DOY

Airborne TMS		Landsat TM		SPOT 4 VEGETATION
Date	DOY	Date	DOY	
		16 February 1997	46	Daily from 30 April to 30 December 1998
		20 March 1997	79	
		21 April 1997	111	
		24 April 1992	114	
		8 June 1997	159	
		11 June 1992	162	
12 August 1997	224	27 June 1992	178	
		13 July 1992	194	
		10 July 1997	222	
		14 July 1992	226	
		12 September 1997	255	
		1 October 1992	274	
		14 October 1997	287	
		2 November 1992	306	
		18 November 1992	322	
Spatial resolution: 3 m		Spatial resolution: 30 m		Spatial resolution: 1000 m

registered to UTM coordinates. A total of 15 Landsat TM images were acquired in 1992 and 1997 over the San Pedro basin area (Table 1). Thematic mapper simulator (TMS) was deployed on an aircraft during the SALSA intensive field campaign in August 1997 (Goodrich et al., 2000) to acquire images at a 3 m spatial resolution. Daily SPOT 4 VEGETATION images were acquired over this study area at a spatial resolution of 1000 m. Therefore, the remotely sensed images had a range of spatial resolution from 3 m to 1 km. In addition to these satellite- and aircraft-based remote sensing data, surface reflectances were also measured at the Audubon ranch near Elgin, AZ, in 1998, using an MMR radiometer in the same spectral bands as Landsat TM sensor.

3.2. Vegetation data

Ground vegetation properties were recorded in 1992, 1997 and 1998 using both destructive sampling technique and Li-Cor's LAI-2000 instrument. Vegetation samples were collected at three study sites. The first site was located in the center of Walnut Gulch Experimental Watershed and the site was dominated by tobosa grasses (*Hilaria mutica*) with some desert shrubs. The second site was near the Lewis Springs within the San Pedro River basin and the dominant grass was sacaton (*Sporobolus wrightii*). The third site was at the Audubon research ranch near Elgin, AZ, and the dominant vegetation types were native upland grasses, Lehmann's lovegrass, and sacaton grasses.

Both destructive and non-destructive methods were used to measure the GLAI. For the destructive method, vegetation samples were collected in the field and brought back to the lab and separated into green vegetation, senescent vegetation, and litter. The single side leaf areas were measured by passing them through an LAI-3000 area meter for each component and GLAI was then computed. For the non-destructive method, LAI-2000 instrument was used to measure total LAI, and the lab-based ratio of green to total leaf areas was used to compute the GLAI. Measurements of the total fractional vegetation cover were made by visual estimate on site during each field visit. Detailed descriptions of this data set can be found in Moran et al. (1998). The ground in situ measurements were then used in this study to examine the effectiveness of the proposed approach.

4. Results

4.1. Spatial dynamics of green vegetation

The spatial distribution of the estimated green vegetation cover and GLAI was derived from the 3 m

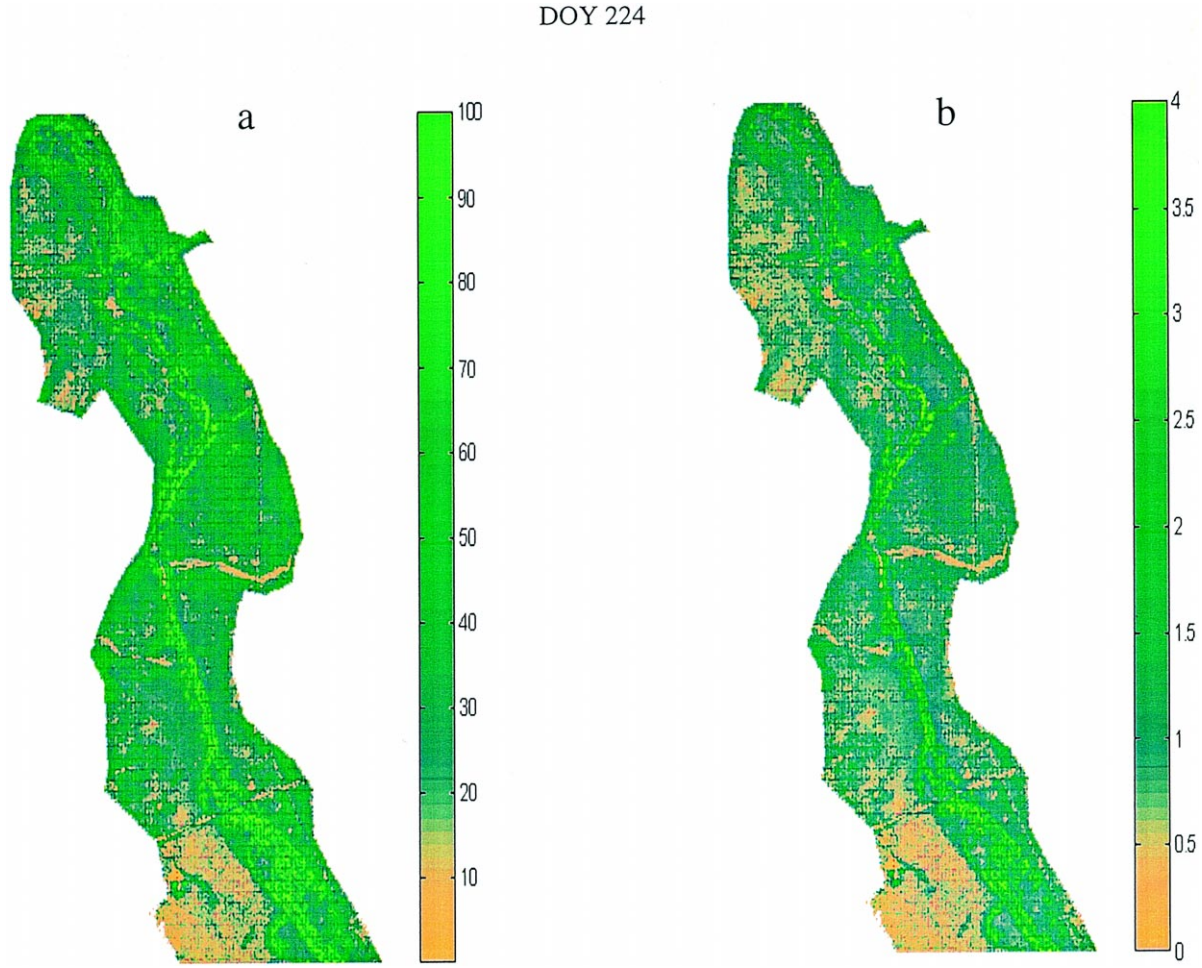

Fig. 2. Spatial distribution of green vegetation cover (a) and GLAI (b) derived from TMS images (3 m resolution) over a portion of the San Pedro basin near the Lewis Springs, AZ.

resolution TMS data (Fig. 2). The spatial extent covered the riparian corridor of the San Pedro River from Hereford to Fairbanks (see Fig. 2 in Goodrich et al., 2000). Dense green vegetation cover was distributed along the river where the cottonwood–willow riparian forest gallery was located. Away from the riverbanks toward the upland areas, the green vegetation cover diminished. There was also a vegetation cover gradient from Fairbanks to Hereford or from north to south of the study area. This gradient was most likely due to water availability from the river and weather pattern variation due to elevation changes. Along the river were cottonwood and willow trees, which require easy access to water. They were the major vegetation community of this riparian corridor that caused evapotranspirative water loss to the atmosphere (Schaeffer et al., 2000; Scott et al., 1999). Away from the river were sacaton grasses and mesquite trees. Although the sacaton grasses were denser than mesquite trees, they did not appear as green as the mesquite trees. This was due to the fact that the senescent sacaton grasses limited the new growth by blocking solar radiation from reaching to the lower layers of the clumps. Therefore, even in the rainy wet season, the sacaton grasses did not appear as green as the cottonwood–willow community and mesquite trees. The fractional green

vegetation cover of the sacaton was thus less than the cottonwood–willow community and mesquite trees.

4.2. Temporal dynamics

To examine the temporal dynamics of vegetation in the San Pedro River basin, a portion of the basin was extracted from two Landsat TM images acquired on 21 April (DOY 111) in the dry season and on 12 September (DOY 255) in the wet season of 1997. The spatial distribution of green vegetation cover (Fig. 3) and GLAI (Fig. 4) of the two seasons covered a portion of the San Pedro River basin. Note the scale difference between Figs. 3 and 4. The Huachuca mountains are located at the lower left corner of the images. The spotty areas with yellow color on the left-hand side of Figs. 3b and 4b were clouds. The dry season was characterized with little green vegetation while the wet season, due to increased precipitation, produced more green vegetation cover. In the dry season, only the river and mountainous areas had green vegetation. In the wet season, cottonwood, willows and mesquite trees were green. The sacaton, in spite of possible new growth underneath the canopy, did not appear green. Due to increased precipitation during the monsoon season, the wet season (Figs. 3b and 4b) had more green vegetation than the dry season (Figs. 3a and 4a).

4.3. Large scale vegetation cover and GLAI

The proposed adjustment approach was applied with SPOT 4 VEGETATION data over a large area that encompassed the San Pedro River basin to demonstrate the application of the approach at different spatial scales. The imagery covered southwest United States and the northern part of Mexico. Eqs. (3) and (4) were applied to the VEGETATION images acquired in both the dry (April) and wet (September) seasons of 1998, and the results are presented in Figs. 5 and 6. Fig. 5 is a map of green vegetation cover derived from SPOT 4 VEGETATION sensor on 21 April and on 12 September 1998, whereas Fig. 6 is the GLAI maps of the two dates. These two maps (Figs. 5 and 6) showed the vegetation patterns of large scales. The coarse spatial resolution f_c maps showed

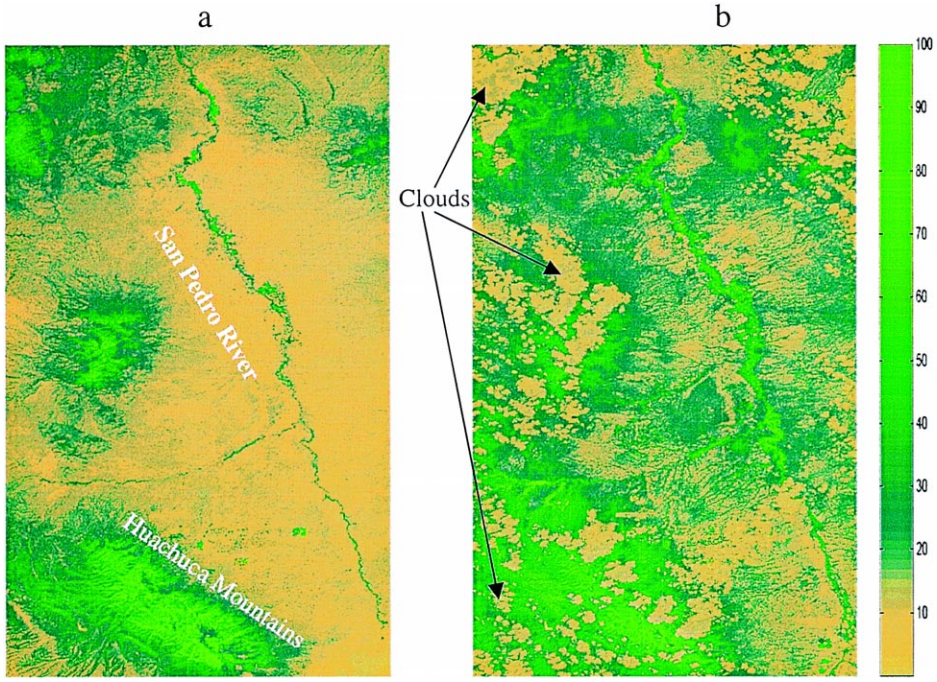

Fig. 3. Green vegetation cover maps derived from TM imagery of: (a) 21 April 1997, DOY 111; (b) 12 September 1997, DOY 255.

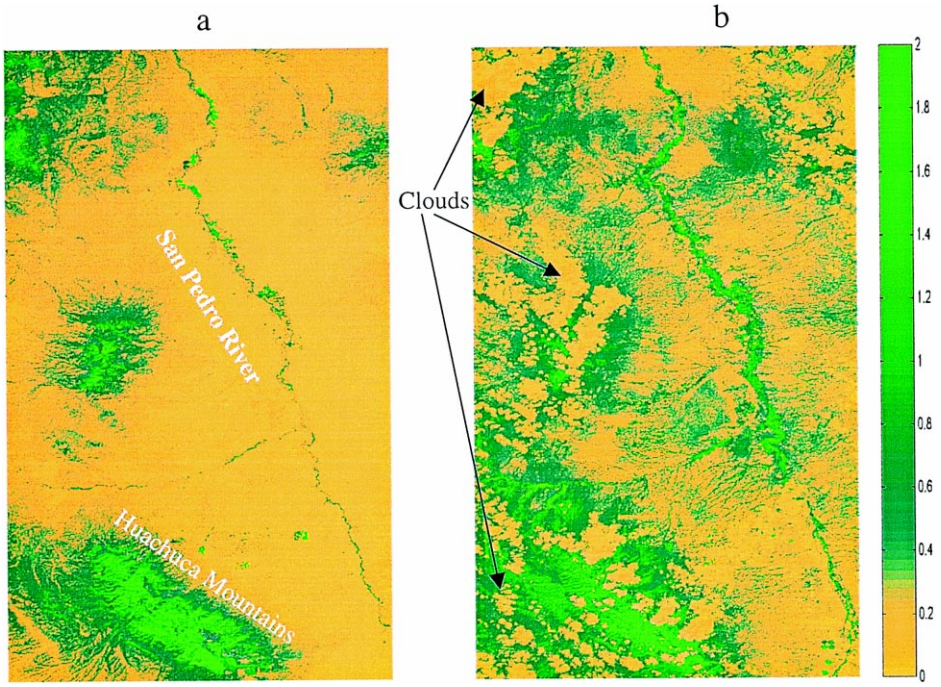

Fig. 4. GLAI maps derived from TM imagery of: (a) 21 April 1997, DOY 111; 12 September 1997, DOY 255.

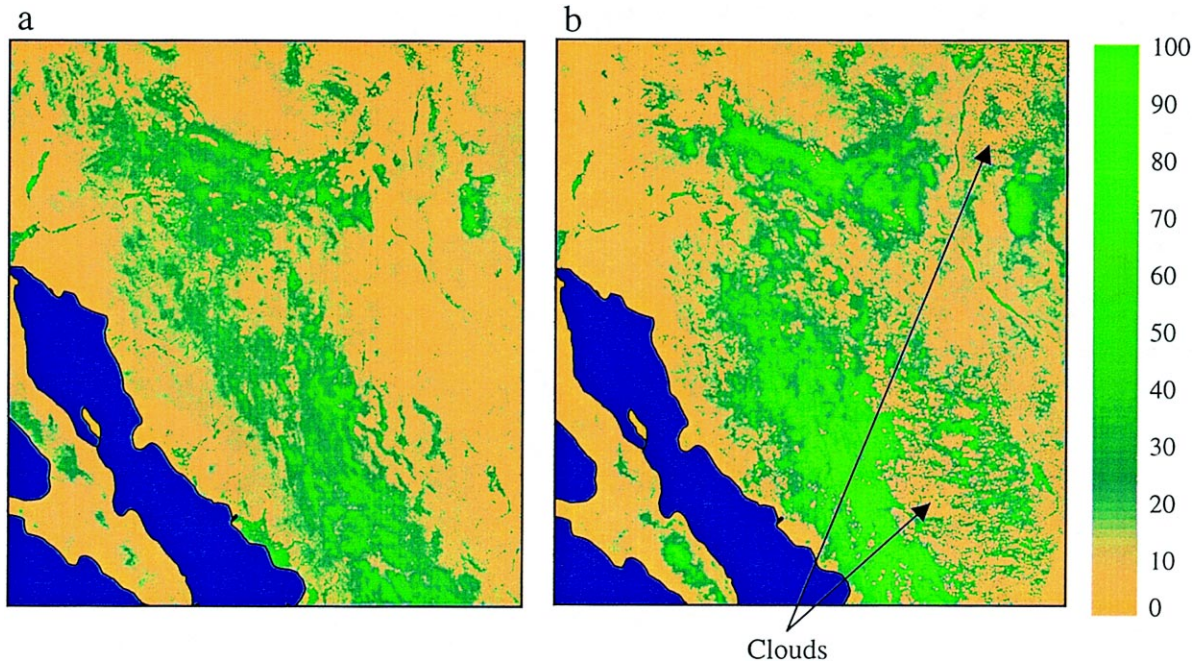

Fig. 5. Green vegetation cover maps derived from SPOT 4 VEGETATION imagery of: (a) 21 April 1998, DOY 111; (b) 12 September 1998, DOY 255.

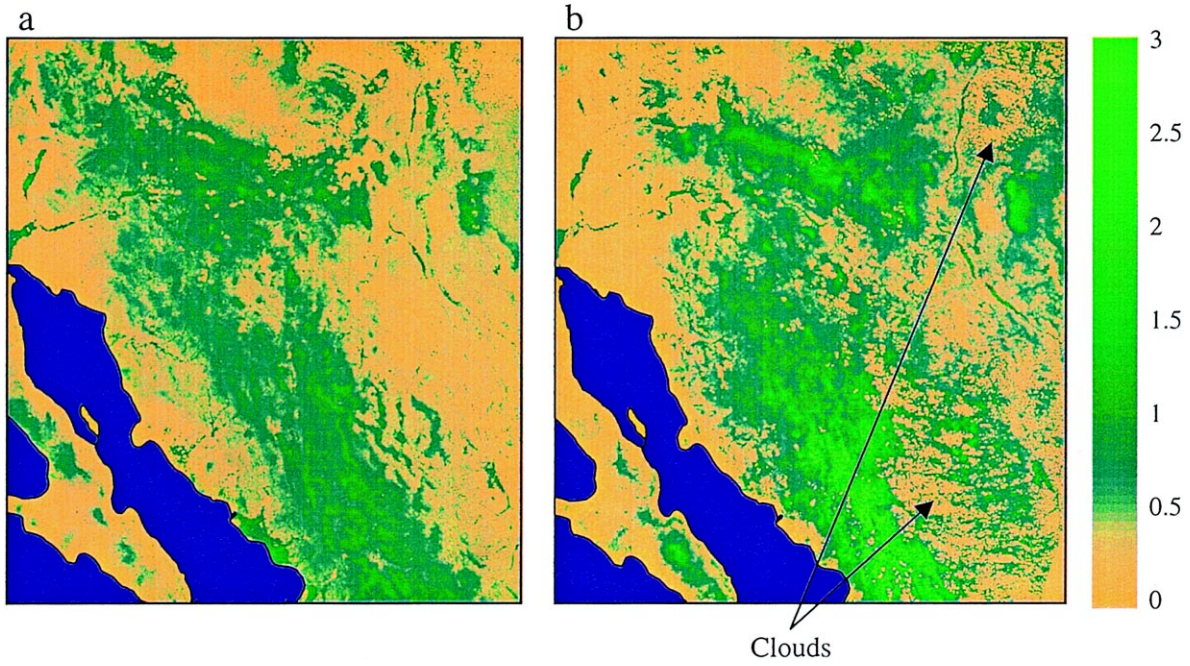

Fig. 6. GLAI maps derived from SPOT 4 VEGETATION imagery of: (a) 21 April 1998, DOY 111; (b) 12 September 1998, DOY 255.

little detailed structures (Figs. 5 and 6) in comparison with those derived from TM images (Figs. 3 and 4). Clearly, the San Pedro River can be seen with TM derived maps (Figs. 3 and 4), but can barely be seen on VEGETATION derived maps in Figs. 5 and 6.

5. Validation

Because of only limited ground-based data available for this study, it was difficult to fully validate the proposed adjustment approach. However, intercomparison of results from different data sets was made in three ways to verify the adjustment approach: (1) intercomparison across atmospheric corrections, (2) intercomparison across spatial scales, and (3) comparison against ground in situ data.

5.1. Across-atmosphere comparison

For this analysis, we selected 1992 TM images because of availability of ancillary data for atmospheric corrections. A window of 9×9 pixels, a size of approximately $270 \times 270\,m^2$ area near Tombstone within the Walnut Gulch Experimental Watershed, was extracted from all 1992 TM images. The mean values of reflectance at the surface (with atmospheric correction) and at the top of atmosphere (without atmospheric correction) were used to compute multitemporal NDVI values. These values were then used in Eqs. (3) and (4) to compute temporal dynamics of f_c and GLAI values without any adjustment. The data without atmospheric correction was then applied to the adjustment approach to investigate its effectiveness on reducing atmospheric effects. The results were plotted as a function of day of year (DOY) in Fig. 7. Without atmospheric correction and OVV adjustment, the temporal dynamics of fractional green cover varied substantially with time and showed little seasonal patterns of vegetation dynamics of the region. After atmospheric corrections, the temporal pattern showed two seasonal variations, with peak-growing season being around DOY of 226 and dry season for the rest of the year. The results obtained with the adjustment approach were similar to the results derived from the atmospherically corrected data and represented the vegetation dynamics of the study area more realistically. The results suggested that the use of OVV

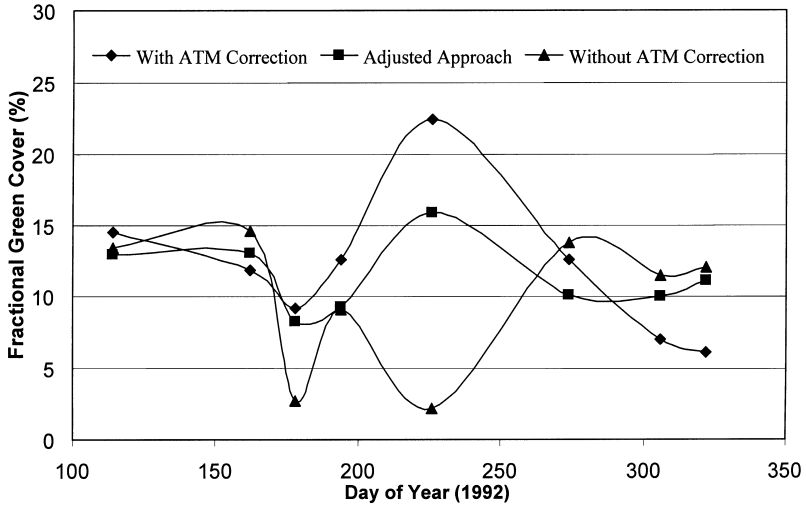

Fig. 7. Comparison of fractional cover values derived with data before and after atmospheric correction, and with the proposed approach using the data without atmospheric correction.

approach could reduce the atmosphere-induced noise in the temporal vegetation dynamics estimated from TM images even though no atmospheric correction was made.

5.2. Across-scale comparison

The remotely sensed data used in this analysis had a range of spatial scales from 3 to 1000 m (Table 1). To compare results across spatial resolutions, a common area ($5 \times 1\,km^2$) found in both TMS (3 m) and TM (30 m) images was extracted and the statistical means were computed. This could not be done with VEGETATION images because the TMS coverage was not enough to cover even a single pixel of the VEGETATION data. To compare spatial scales between TM and VEGETATION, a separate common area ($5 \times 5\,km^2$) was extracted and statistical means were used for intercomparison. Due to limited TMS data, we could only compare TMS with TM for the wet season, while comparison between TM and VEGETATION was made for both dry and wet season. The results were plotted in Fig. 8. Although the spatial scales were different, the mean values of the fractional green cover estimated at three spatial scales agreed well. Because the TMS image was acquired over the intensive study site at the Lewis Springs site of SALSA program and had a spatial resolution of 3 m, we felt quite confident about the f_c estimate with this image. Therefore, the estimated f_c from the fine resolution TMS image could be used to assess the accuracy of f_c estimates by the coarser resolution TM and VEGETATION images. The good agreement among all three scales (Fig. 8) suggest that the estimated f_c with TM and VEGETATION images had approximately the same accuracy of that estimated by TMS image.

5.3. Comparison with in situ measurements

In this analysis, we selected 1997 TM images because of availability of ground in situ measurements of fractional cover and GLAI from the SALSA program and other research projects at the three study sites described previously. The estimated f_c and GLAI values for this analysis were all derived from 1997 TM images without atmospheric corrections to demonstrate the effectiveness of the adjustment approach for reducing atmospheric perturbation. Because of rigid Landsat satellite overpass schedules over the study sites, the ground in situ measurements were not always coincident with the satellite overpass dates.

The results from the Lewis Springs (sacaton grasses) in the San Pedro River basin and the Walnut Gulch Experimental Watershed (tobosa grasses) were

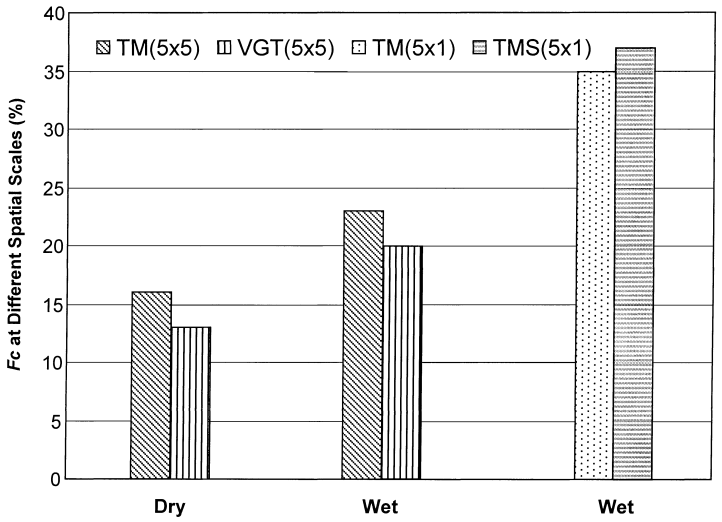

Fig. 8. Comparison of fractional green cover estimated using the proposed approach at different spatial scales: 3 m (TMS), 30 m (TM) and 1000 m (VEGETATION).

presented in Fig. 9. The in situ f_c values agreed reasonably well with those derived from TM images. The seasonal trends of the estimated f_c were reasonably well in agreement with those observed on the ground. In spite of the fact that there was a good agreement between estimated f_c values and in situ measurements, no conclusive statements could be made, due to limited number of data available for this analysis.

For the Audubon study site, both fractional green cover (f_c) and GLAI values were derived using ground-based reflectance measurements with the adjustment approach. The computed f_c and GLAI values were compared with in situ measurements in Fig. 10. The estimated fractional green cover agreed reasonably well with ground measurements in the early growing season. On DOY 216, the fractional green

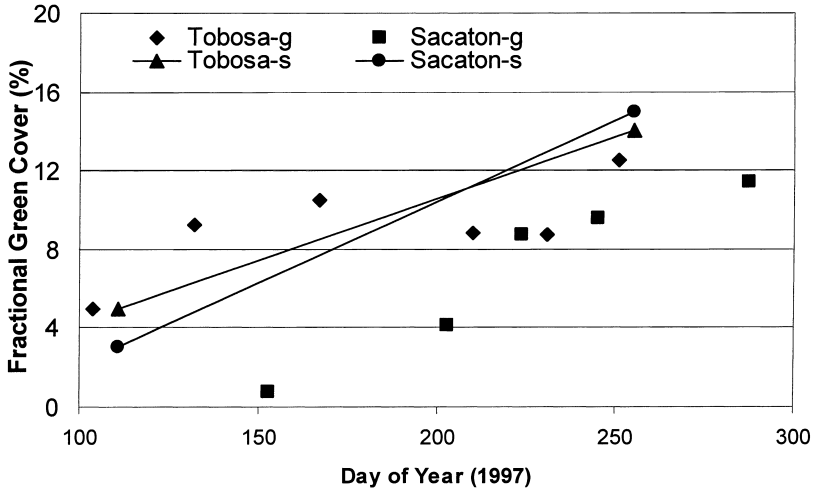

Fig. 9. Comparison of ground-based green vegetation covers (as indicated with a suffix g) with those estimated using satellite imagery (as indicated with suffix s) for tobosa and sacaton grasses using the proposed approach.

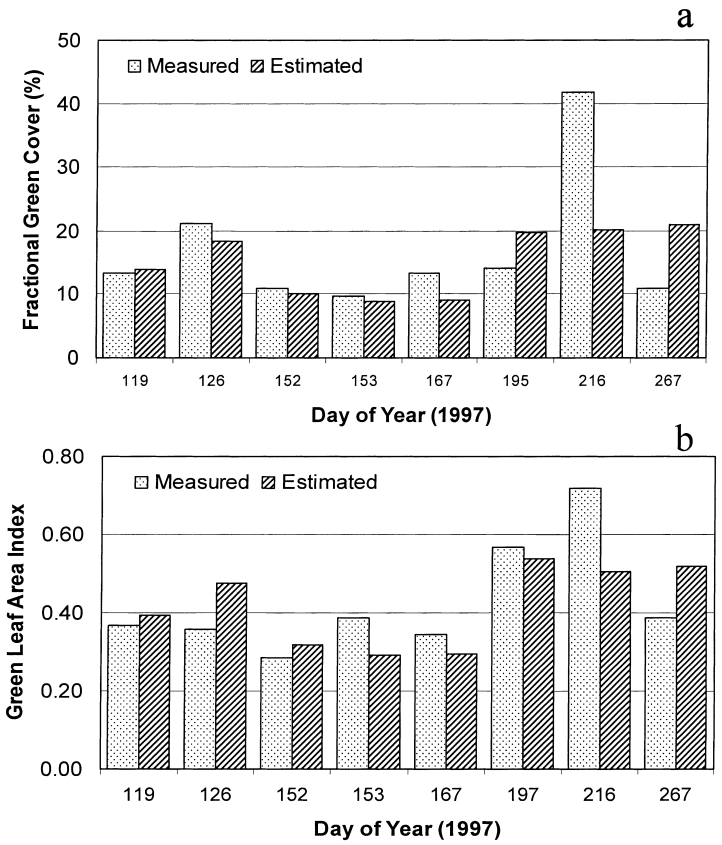

Fig. 10. Comparison of in situ fractional green cover (a) and GLAI (b) measurement with those derived using the proposed approach and ground-based reflectance measurements at Audubon site, where native grasses and Lehmann lovegrass were dominant species.

vegetation cover, f_c, was underestimated by approximately 50%. This unexpected discrepancy on this date could be due to several factors. One was the heterogeneous nature of the study areas. Since ground sampling was made within several $2 \times 2\,m^2$ blocks, the averaged values may not represent what a sensor would 'see' with a footprint of $30 \times 30\,m^2$ area. The estimated GLAI, agreed reasonably well with in situ measurements. It should be pointed out that there were uncertainties associated with ground GLAI measurements. The uncertainty in the in situ GLAI measurements could result from spatial variation of the vegetation density, random errors of the equipment used, and measurement condition variations when using LAI-2000 instrument, resulting in discrepancies between in situ measurements and remote estimates.

6. Discussion

The results presented here are preliminary. The remotely estimated f_c and GLAI were compared with ground-based measurements using a limited data set. Further validation of the results from this study is needed in order to assess the accuracy of the adjustment approach. This would require carrying out extensive ground measurements at varying spatial and temporal scales with coincident satellite overpasses. Furthermore, a scaling up scheme for f_c and GLAI variables needs to be developed in order to conduct a thorough validation of the proposed approach.

The use of the $NDVI_{veg} = 0.8$ in Eq. (3) was specific to the research area and was independent of vegetation types. This upper boundary may vary with vegetation types within the area of interest. Use of

this approach for other vegetation types may require knowledge of this boundary condition. Furthermore, the equation used to compute GLAI was developed for desert grasslands in arid and semi-arid regions. The use of this equation for other vegetation types such as dense agricultural crops needs further investigation.

The OVVs selected for this study were the bare soils of Wilcox playa in southern Arizona and White Sands, New Mexico, which resulted in a valid assumption that no vegetation was present all year round. When working with other data sets of different spatial resolution, one may find other invariant objects to be more suitable. However, it should be pointed out that the OVVs should be large enough to encompass at least a few pixels. For remotely sensed imagery such as Landsat TM, a field of bare soil may prove to be sufficient for this purpose.

Although a dynamic baseline adjustment factor, derived from OVV, was used to circumvent atmospheric effects found in most remotely sensed, no consideration was given to the effect of atmosphere on the dynamic range of NDVI values. As shown in other studies, the atmosphere could reduce NDVI dynamics by as much as 10% (Qi et al., 1994), which would result in errors in f_c and GLAI estimation. Quantitative assessment of atmospheric and bidirectional effects on the dynamics of vegetation indices, and on the f_c and GLAI estimation need to be further investigated.

Finally, Eqs. (3) and (4) did not specify the vegetation types. Because different types of vegetation tend to result in variable NDVI dynamics, use of these equations for remotely sensed imagery of multi-vegetation types may result in a constant bias towards some vegetation types. Therefore, uncertainties in estimated f_c and GLAI associated with multiple vegetation types needs to be quantified. When applying these two equations for large-scale remote sensing images, it may be a good exercise to classify the imagery first and then use variable upper boundaries for different classes.

Acknowledgements

Financial support from the VEGETATION project at the USDA–ARS Water Conservation Laboratory, the VEGETATION project at CIRAD-GEOTROP, Montpellier, FRANCE, USDA–ARS Global Change Research Program, NASA grant W-18, 1997, NASA Landsat Science Team, grant #S-41396-F and NASA IDP-88-086 are acknowledged. Assistance was also provided in part by the NASA/EOS grant NAGW2425. Support from the NSF-STC SAHRA (sustainability of semi-arid hydrology and riparian areas) under agreement No. EAR-9876800) is also gratefully acknowledged. Special thanks are extended to the ARS staff located in Tombstone, AZ for their diligent efforts and to USDA–ARS Weslaco for pilot and aircraft support.

References

Caselles, V., Garcia, M.J.L., 1989. An alternative approach to estimate atmospheric correction in mulit-temporal studies. Int. J. Remote Sensing 10 (6), 1127–1134.

Chavez Jr., P.S., 1988. An improved dark-object subtraction technique for atmospheric scattering correction of multispectral data. Remote Sensing Environ. 24, 459–479.

Goodrich, D.C., Chehbouni, A., Goff, B., MacNish, B., Maddock III, T., Moran, M.S., Shuttleworth, W.J., Williams, D.G., Watts, C., Hipps, L.H., Cooper, D.I., Schieldge, J., Kerr, Y.H., Arias, H., Kirkland, M., Carlos, R., Cayrol, P., Kepner, W., Jones, B., Avissar, R., Begue, A., Bonnefond, J.M., Boulet, G., Branan, B., Brunel, J.P., Chen, L.C., Clarke, T., Davis, M.R., DeBruin, H., Dedieu, G., Elguero, E., Eichinger, W.E., Everitt, J., Garatuza-Payan, J., Gempko, V.L., Gupta, H., Harlow, C., Hartogensis, O., Helfert, M., Holifield, C., Hymer, D., Kahle, A., Keefer, T., Krishnamoorthy, S., Lhomme, J.P., Lagouarde, J.P., Lo Seen, D., Laquet, D., Marsett, R., Monteny, B., Ni, W., Nouvellon, Y., Pinker, R.T., Peters, C., Pool, D., Qi, J., Rambal, S., Rodriguez, J., Santiago, F., Sano, E., Schaeffer, S.M., Schulte, S., Scott, R., Shao, X., Snyder, K.A., Sorooshian, S., Unkrich, C.L., Whitaker, M., Yuce, I., 2000. Preface paper to the Semi-Arid Land-Surface-Atmosphere (SALSA) Program Special Issue. Agric. For. Meteorol. 105, 3–19.

Kaufman, Y.J., Tanre, D., 1992. Atmospherically resistant vegetation index (ARVI) for tos-MODIS. IEEE Trans. Geosci. Remote Sensing, 30 (2), 261–270.

Kepner, W.G., Watts, C.J., Edmonds, C.M., Arias, H.M., 1998. A Landscape Approach for Evaluating Ecological Risk in a Semi-arid Environment. Arizona Hydrological Society, Tucson, AZ, September 23–26, 1998.

Maas, S., 1998. Estimating cotton canopy ground cover from remotely sensed scene reflectance. Agron. J. 90, 384–388.

Moran, M.S., Jackson, R.D., Clarke, T.R., Qi, J., Cabot, F., Thome, K.J., Markham, B.N., 1996. Reflectance factor retrieval from Landsat TM and SPOT HRV data for bright and dark targets. Remote Sensing Environ. 52, 218–230.

Moran, M.S., Clarke, T.R., Qi, J., et al., 1997. Practical techniques for conversion of airborne imagery to reflectances. In: Proceedings of the 16th Biennial Workshop on Color

Photography and Videography in Res. Assessment, Weslaco, TX, April 29, 1997.

Moran, M.S., Williams, D., Goodrich, D.C., Chehbouni, A., Begue, A., Boulet, G., Cooper, D., Davis, R.G., Dedieu, G., Eichinger, W., 1998. Overview of remote sensing of semi-arid ecosystem function in the upper San Pedro River basin, Arizona. In: Proceedings of the American Meteorology Society, Phoenix, AZ, January 11–16.

Qi, J., Kerr, Y., Chehbouni, A., 1994. External factor consideration in vegetation index development. Papers presented at the Sixth International Symposium on Physical Measurements and Signatures in Remote Sensing, Val d'Isere, France, January 17–21, 1994.

Qi, J., Kerr, Y., Moran, M.S., Weltz, M., Huete, A.R., Sorooshian, S., Bryant, R., 2000. Leaf area index estimates using remotely sensed data and BRDF models in a semi-arid region. Remote Sens. Environ. 73, 18–30.

Schaeffer, S.M., Williams, D.G., Goodrich, D.C., 2000. Transpiration of cottonwood/willow forest estimated from sap flux. Agric. For. Meteorol. 105, 257–270.

Schott, J., Salvaggio, R.C., Volchok, W.J., 1988. Radiometric scene normalization using pseudoinvariant features. Remote Sensing Environ. 26, 1–16.

Scott, R.L., Shuttleworth, W.J., Goodrich, D.C., Maddock III, T., 1999. The water use of two dominant vegetation communities in a semi-arid riparian ecosystem. Agric. For. Meteorol. 105, 241–256.

Watts, C.J., Kepner, W.G., Edmonds, C.M., Arias, H.M., 1998. Landscape Change in the Upper San Pedro Watershed. Arizona Hydrological Society, Tucson, AZ, September 23–26, 1998.

Zeng, X., Dickinson, R.E., Walker, A., Shaikh, M., DeFries, R.S., Qi, J., 2000. Derivation and evaluation of global 1-km fractional vegetation cover data for land modeling. J. Appl. Meteorol. 39 (6), 826.